Preparation of chitosan/amine modified diatomite composites and adsorption properties of Hg(II) ions

Yong Fu, Yue Huang, Jianshe Hu and Zhengjie Zhang

ABSTRACT

A green functional adsorbent (CAD) was prepared by Schiff base reaction of chitosan and amino-modified diatomite. The morphology, structure and adsorption properties of the CAD were characterized by Fourier transform infrared spectroscopy, thermogravimetric analysis, scanning electron microscopy and Brunauer Emmett Teller measurements. The effect of pH value, contact time and temperature on the adsorption of Hg(II) ions for the CAD is discussed in detail. The experimental results showed that the CAD had a large specific surface area and multifunctional groups such as amino, hydroxyl and Schiff base. The optimum adsorption effect was obtained when the pH value, temperature and contact time were 4, 25 °C and 120 min, respectively, and the corresponding maximum adsorption capacity of Hg(II) ions reached 102 mg/g. Moreover, the adsorption behavior of Hg(II) ions for the CAD followed the pseudo-second-order kinetic model and Langmuir model. The negative ΔG^0 and ΔH^0 suggested that the adsorption was a spontaneous exothermic process.

Key words | adsorption, amino-modified diatomite, chitosan, Hg(II) ions

Yong Fu
Yue Huang
Jianshe Hu (corresponding author)
Center for Molecular Science and Engineering,
College of Sciences,
Northeastern University,
Shenyang 110819,
China
E-mail: *hujs@mail.neu.edu.cn*

Zhengjie Zhang
Zhong Ke Jing Tou Environmental Technology
(Jiang Su) Co., Ltd,,
Yancheng 224001,
China

INTRODUCTION

Due to the development of modern industry, a large number of mercury ion pollutants have been discharged into the water environment. Mercury ions are latent, difficult to degrade, easy to enrich, can enter the human body through the food chain and ultimately endanger human health (Cho *et al.* 2012; Awual *et al.* 2016), causing kidney and brain damage, resulting in central nervous system and endocrine disorders (Naushad *et al.* 2015). In heavy metal pollution, such as Cd(II) (Chen *et al.* 2014; Xu *et al.* 2017), Ni(II) (Sun *et al.* 2017), Hg(II) (Cheng & Hu 2012; Carter *et al.* 2014) and so on, the problem of mercury ion pollution in the water is more prominent. Today, water is an important and rare resource, so it is very important to solve the mercury ion pollution of surface water and groundwater (Khraisheh *et al.* 2004).

Up to now, many treatment methods have been applied to deal with mercury ion wastewater, such as chemical precipitation (Charerntanyarak 1999), electro-dialysis (Amor *et al.* 2001), and adsorption (Li *et al.* 2014). Over the past decades, the adsorption method has become an important and effective purification and separation technology in wastewater treatment (Al-Ghouti *et al.* 2004). Many adsorbents such as activated carbon (Kadirvelu *et al.* 2001), synthetic resins (Demirbas *et al.* 2005), natural or synthetic zeolites (Bailey *et al.* 1999), natural or modified diatomite (Wu *et al.* 2005) have been used to remove heavy metal ions in the water, in which modified diatomite has become a promising adsorbent because of its unique physical and chemical properties, low cost and efficient removal of heavy metal ions (Sheng *et al.* 2009).

It is known that diatomite has a large number of natural, ordered pores and large specific area; in addition, the surface of diatomite and the inner surface of the pores are distributed with a large amount of silicon hydroxyl groups and negative charge (Yu *et al.* 2012). Due to its distinctive structure and chemical properties, diatomite with proper modification has strong adsorbability, which makes it a very promising adsorption material (Bello *et al.* 2014).

Chitosan (CS) is a new kind of natural macromolecule material; it contains a variety of active functional groups such as hydroxyl, amino group and glycosidic bond in the molecule, which makes it form a coordination bond with metal ions through chelate effect. CS has a stronger adsorption capacity for heavy metal ions, such as Hg(II) (Caner *et al.* 2015), Pd(II) (Fan *et al.* 2013), Cr(VI) (Etemadi *et al.* 2017), Ni(II) (Reddy & Lee 2013) and so on, which has

doi: 10.2166/wst.2018.018

been paid more and more attention and become a hotspot in the past 10 years.

APTES (3-aminopropyltriethoxysilane) is an organic coupling agent, which contains silicon and amino in the molecular structure. The siloxy group is easily hydrolyzed to form -C-Si-O- bonds with hydroxyl group-containing carrier materials, and the amino group is grafted onto the surface of the carrier material, which can be chemically bonded with the organic and inorganic materials to increase the adhesion of two materials; as a result, the surface of the inorganic materials is modified with the amino functional group (Gökalp *et al.* 2016). Amino functional groups have a strong ability to chelate heavy metals; some researches showed that the inorganic adsorbent after being aminated had a strong adsorption and separation ability to the heavy metal ions (Qiao *et al.* 2015).

In the present work, we aimed to design and prepare a kind of green functional adsorbent (CAD) with high adsorption capacity and stable structure. First, fine diatomite was obtained by pickling and high temperature calcination, and then the diatomite was organized by APTES. As a result, the modified diatomite (DE-NH_2) had a good affinity with CS. In addition, DE-NH_2 and CS were connected through the Schiff base reaction with glutaraldehyde as a bridge. Compared with the conventional composite adsorbents, CAD not only had a high removal rate and adsorption capacity of the adsorbent, but also improved the acid resistance of the adsorbent. The morphology, structure and adsorption properties of the CAD were investigated using Fourier transform infrared (FT-IR) spectroscopy, thermogravimetric analysis (TG) scanning electron microscope (SEM) and Brunauer Emmett Teller (BET) measurements. CAD, as an adsorbent of Hg(II) ions, was systematically studied to explore the effects of adsorption factors such as the pH of the solution, contact time and temperature. The schematic depiction of the CAD is illustrated in Figure 1.

MATERIALS AND METHODS

Materials

All chemicals and materials were obtained from the indicated sources. Chitosan (CS, 85% deacetylated) was purchased

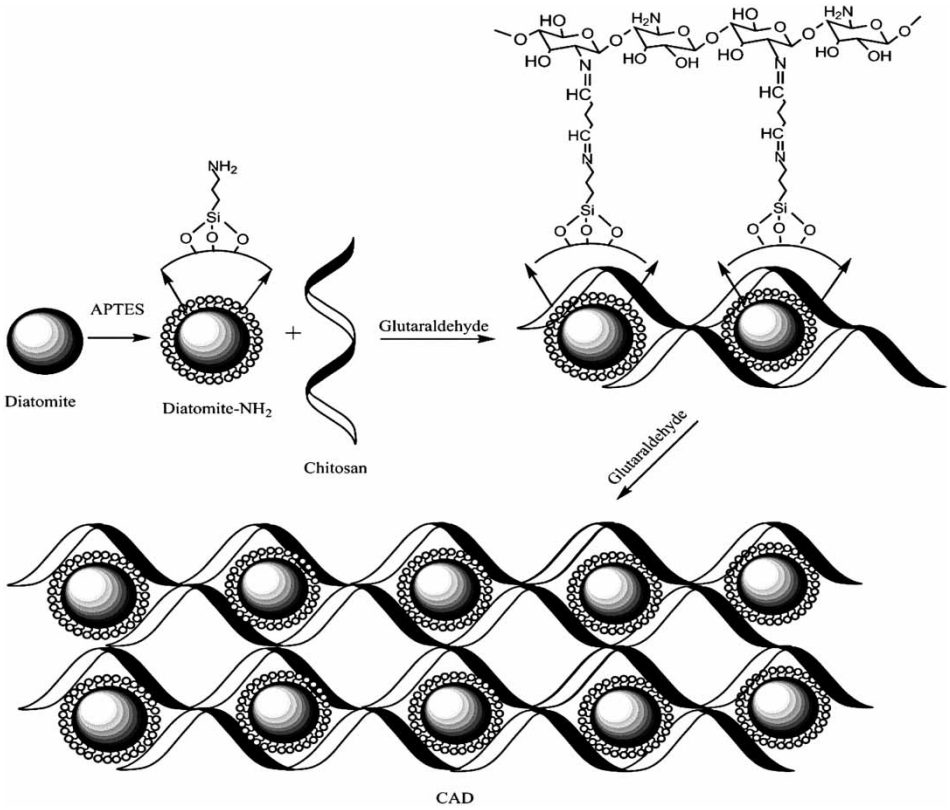

Figure 1 | Schematic depiction of the formation of the CAD.

from Qingdao Baicheng Biochemical Co. (China). The raw diatomite (92.8% SiO_2, 4.2% Al_2O_3, 1.5% Fe_2O_3, and other metal oxides) were purchased from Jilin Kaida Diatomite Co. Ltd (China). APTES was purchased from Nanjing Forward Chemical Co. (China). Glutaraldehyde (25%) was purchased from Damao Chemical Agent Company (Tijin, China). Mercurium nitrate was purchased from Guizhou Tongren Tailuier chemical plant. All other solvents and reagents used were purified by standard methods.

Characterization

FT-IR spectra were recorded using a KBr pellet in the range of 400–4,000 cm^{-1} on a PerkinElmer spectrum One (B) spectrometer (Foster City, CA). The morphology was observed by scanning electron microscope (SEM, JEOL 6500F, Japan). Thermal decomposition temperature was measured under nitrogen atmosphere with a Netzsch 209C (Hanau, Germany) (TG) at a heating rate of 20 °C/min. The BET surface area and the pore size distribution were measured using N_2 adsorption and desorption (Quadrasorbsi, Quantachrome, USA) at 77 K. The mercury ion concentration was measured by a TU-1901 dual-beam UV-vis spectrophotometer (Beijing Purkinje General Instrument Co., Ltd, China) with a range of 450–600 nm.

Preparation of CS/amine functional diatomite composites (CAD)

Firstly, the diatomite powder (200 mesh) was treated with 40% sulfuric acid at a solid-liquid ratio of 1: 4, The mixture was mechanically stirred at 80 °C for 8 h, then filtered and washed several times with distilled water, dried in the vacuum oven at 60 °C for 24 h, transferred to a muffle furnace and calcined at 450 °C for 6 h. DE was obtained. Secondly, DE (4 g) was added to a round bottom flask with 80% ethanol solution (50 ml), and ultrasonically dispersed for 60 min. APTES (2 ml) was slowly added dropwise to the round bottom flask under nitrogen, the mixture was strongly magnetically stirred at 45 °C for 12 h, washed with ethanol, filtered and dried *in vacuo* at 45 °C for 24 h. DE-NH_2 was prepared. DE-NH_2 (2 g) was added to a round bottom flask with 2% acetic acid solution (80 ml) and mechanically stirred at room temperature, CS (0.8 g) was added slowly to the mixture under constant stirring, then 1% glutaraldehyde solution (2.36 ml) was slowly added dropwise to the mixture and stirred at 45 °C for 6 h. The pH of the mixture was adjusted with 2% sodium hydroxide until it reached 7, transferred to the fridge for freezing for 24 h, frozen at room temperature for 12 h, washed several times with distilled water, filtered and dried at 45 °C for 24 h. Finally, the obtained product was ground into powder (100 mesh) and sealed as CAD.

Adsorption experiments

Batch adsorption experiments were conducted using the CAD as an adsorbent. A series of preliminary experiments were conducted to study the optimum pH of the solution, sorbent dosage, contact time and temperature. Specific experimental operation is as follows: 100–300 mg/L $Hg(NO_3)_2$ standard solution was configured, poured into a volume of 250 mL beaker and a certain amount of adsorbent added. The pH of the solution was adjusted from 1 to 6 by 0.8 mol/L nitric acid solution, with contact time varying from 0 to 120 min and magnetic stirring at different temperatures. The concentration of Hg(II) ions in the solution after adsorption was measured by using dithizone spectrophotometry, according to Equation (1), to calculate the adsorption amount of the CAD on Hg(II) ions.

$$q_e = \frac{(C_0 - C_e) \cdot V}{m} \tag{1}$$

$$\text{Removal efficiency } (\%) = \frac{(C_0 - C_e)}{C_0} \cdot 100\% \tag{2}$$

where C_0(mg/L) and C_e(mg/L) are the initial and equilibrium concentrations of Hg(II) ions, V(L) is the volume of Hg(II) ion solution, m(g) is the weight of the CAD used and q_e(mg/g) is the adsorption amount. All batch experiments conducted in this study were repeated twice to make sure of the accuracy and reproducibility of the experimental data.

RESULTS AND DISCUSSION

Characterization of CAD

FT-IR analysis

Figure 2(a) shows the FT-IR spectra of DE, DE-NH_2 and CAD. The FT-IR spectra of DE show the characteristic peaks at 3,650, 1,090 and 800 cm^{-1} belonged to Si-OH of stretching vibration, Si-O anti-symmetrical stretching vibration and Si-O symmetrical stretching vibration. The FT-IR spectra of DE-NH_2 show the peaks at 3,450, 1,637 and 691 cm^{-1} correspond to N-H stretching vibration peak,

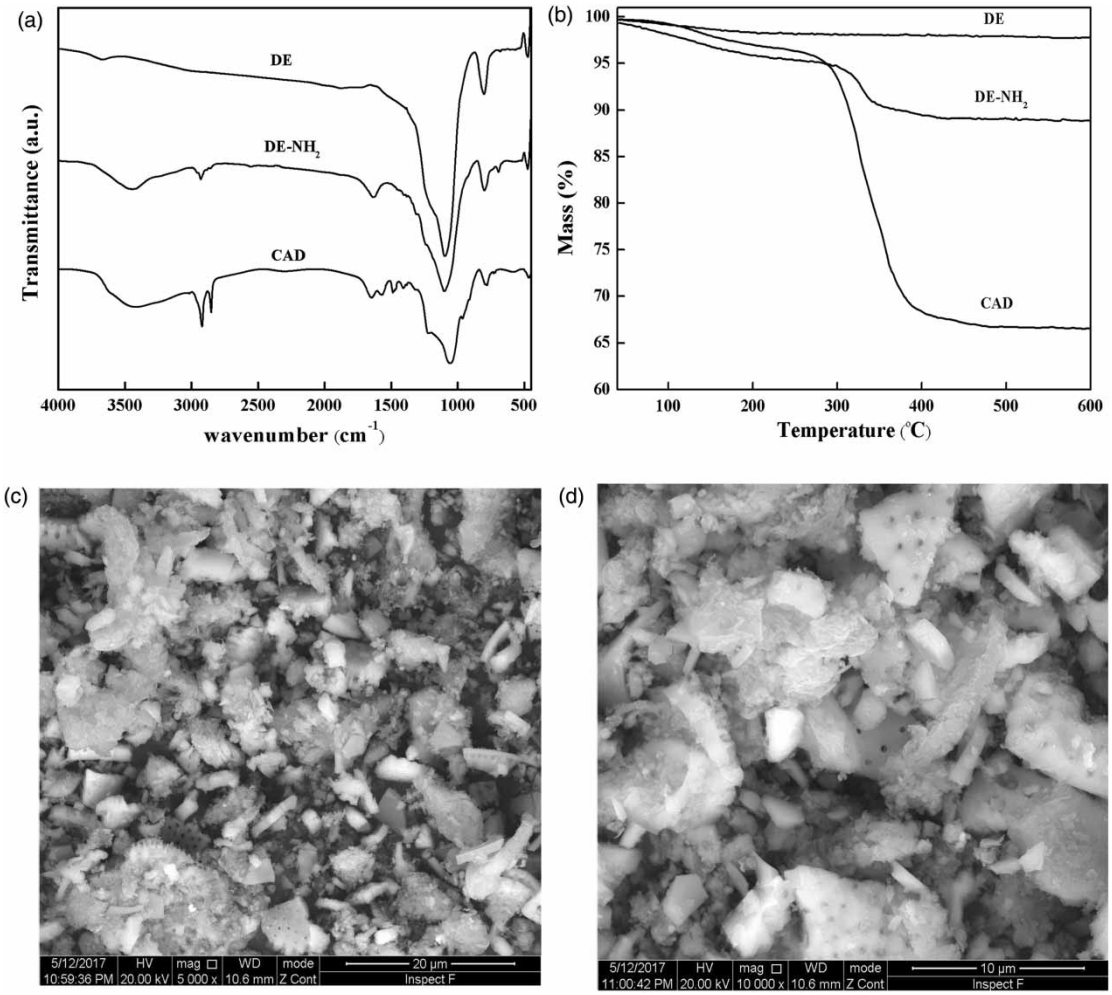

Figure 2 | FT-IR spectra of DE, DE-NH_2 and CAD (a); TG curves of DE, DE-NH_2 and CAD (b) and SEM images of CAD (c), (d).

N-H shear vibration peak and N-H non-planar bending vibration peaks, the stretching vibration band observed at 2,938 cm^{-1} was the C-H stretching vibration peak, which indicated that the amino group had been successfully modified to the surface of DE. The FT-IR spectra of CAD indicates the broad peak at about 3,435 cm^{-1} is the multiple absorption peak formed by the O-H stretching vibration absorption peak and the N-H stretching vibration absorption peak, the peaks at 1,596, 1,560 and 1,340 cm^{-1}, attributed to the N-H bending of CS, C = N stretching vibration and the C-O stretching vibration, indicating that a Schiff base was generated.

TG analysis

TG curves of DE, DE-NH_2 and CAD are shown in Figure 2(b). It can be observed that the first degradation stage of all curves lost water physically adsorbed on the surface at the range of 40–150 °C. According to the curve of DE, the weight loss (1–2%) at the range of 40–150 °C is the evaporation of physisorbed water and the other stage of the weight loss remained essentially unchanged, indicating that refined diatomite is relatively stable and pure. Based on the curve of DE-NH_2, the weight loss (7–8%) in the range of 150–450 °C is decomposition of the organic group modified on the surface of diatomite, which can be explained by the amino group successfully being modified to diatomite. From the curve of CAD, the weight loss (30–31%) observed at the range of 150–600 °C is the decomposition of organic groups modified on the surface of diatomite and CS.

SEM analysis

Figure 2(c) and 2(d) shows SEM images of CAD with magnifications of 5,000 and 10,000, respectively. Figure 2(c)

manifests that white strip of CS dispersed evenly in the DE-NH_2. Figure 2(d) shows DE is mainly disc algae, and the shell wall is mesh with many small pores. The surface of CS became rough, indicating that that cross-linking and Schiff base reaction occurred. It could be seen that CS and DE-NH_2 had good adhesion together.

Analysis of specific surface area and pore structure

The pore volume (V_{total}, cm^3/g), pore size (D_{BJH}, nm) and specific surface area (S_{BET}, m^2/g) of DE, DE-NH_2 and CAD are listed in Table 1 by using N_2 physisorption techniques at 77 K.

According to Table 1, the specific surface area, the pore volume and size of DE-NH_2 are smaller than DE, this is mainly due to the reaction of APTES with the hydroxyl groups inside the DE pores, making the volume and size smaller, which suggests that the amino groups have been successfully modified to the surface of the DE. The specific surface area and average pore volume of CAD are bigger than DE-NH_2, because CS was crosslinked with glutaraldehyde to form some new pores.

Effect of pH value on adsorption

The pH of the solution is an important factor affecting the removal efficiency and adsorption capacity. The experiments were carried out by controlling pH value from 1 to 6, which ensured that Hg(II) ions were present totally in ionic states. The results are shown in Figure 3.

With the pH value increasing from 1 to 4, the adsorption capacity quickly increased and reached maximums at pH 4, then adsorption capacity began to gradually reduce. Therefore, the optimum pH for CAD is 4. The reason is that silica hydroxyl of DE in the aqueous solution could produce a certain negative charge by the dissociation of H^+, which reacts with Hg(II) ions according to the following reaction (Equation (3)):

$$(DE) - O^- + H^+ \leftrightarrow (DE) - OH \quad (3)$$

Table 1 | Pore volume, pore size and surface area of DE, DE-NH_2 and CAD

Sample	Pore volume (cm^3/g)	Pore size (nm)	Surface area (m^2/g)
DE	0.12201	14.9515	7.7044
DE-NH_2	0.0153	3.3099	5.8149
CAD	0.1094	3.9336	15.0052

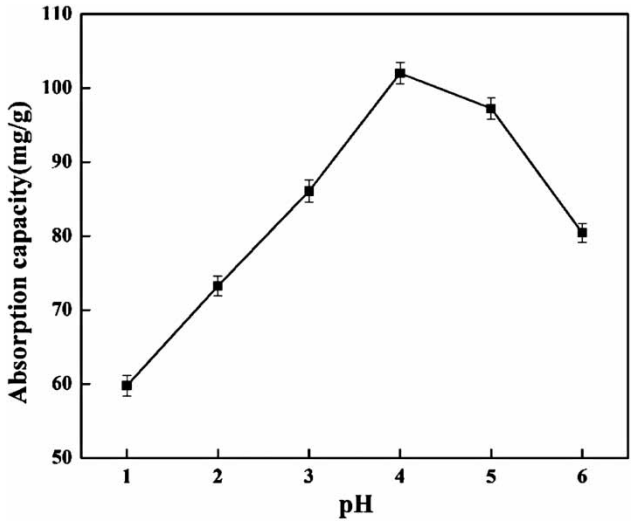

Figure 3 | Effect of pH on the sorption of Hg(II) ions (200 mg/L initial Hg(II) ions concentration, 100 ml; CAD, 0.15 g; temperature, 25 °C; time, 120 min).

However, if the pH of the solution was too low and a large amount of H^+ was present, this reduced the dissociation of the hydroxyl groups on the surface of diatomaceous earth. In addition, the amine groups are bound by H^+ and lose the chance of binding to Hg(II) ions, resulting in a decrease in the adsorption capacity according to the following reaction (Equation (4)):

$$(CAD) - NH_2 + H^+ \leftrightarrow (CAD) - NH_3^+ \quad (4)$$

At high pH (pH > 4), with the pH value increasing, the adsorption capacity gradually decreases because the Hg(II) ions hydrolyze into complexes and $Hg(OH)_2$ is formed (Yu *et al.* 2012). The formed mercury hydroxide precipitated on the surface of the CAD and prevented further adsorption, So the pH of the solution is below 6.

Effect of contact time and temperature

Adsorption experiments were conducted to investigate the time dependency of Hg(II) ion uptake; the results are shown in Figure 4.

It could be seen that the adsorption capacity increased with increasing contact time and reached a maximum at 120 min, and then kept almost unchanged. Therefore, 120 min is determined as the optimum contact time. To assess the role of temperature on the extraction of Hg(II) ions by CAD, the adsorption experiments were carried out at 25, 35 and 45 °C. Figure 4 also illustrates that the adsorption

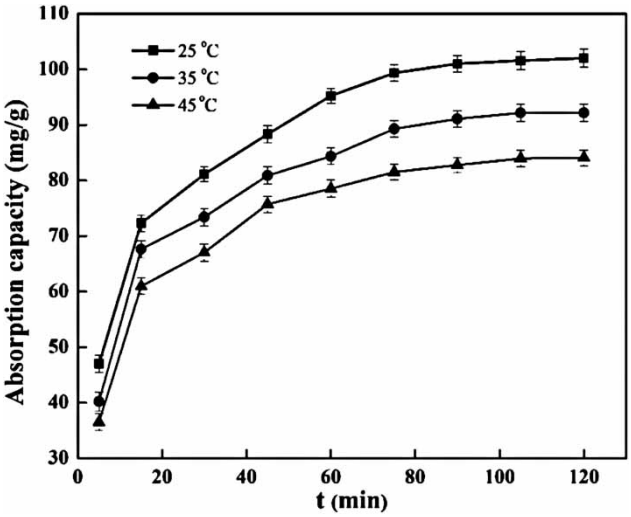

Figure 4 | Effect of contact time and temperature on the sorption of Hg (II) ions (200 mg/L initial Hg(II) ions concentration, 100 ml; CAD, 0.15 g; pH, 4; time, 120 min).

capacity reduced from 102 to 84 mg/g with increasing temperature from 25 to 45 °C, which proved that the uptake process of the Hg(II) ions was exothermic in nature.

Effect of sorbent dosage

The effect of the dosage on the adsorption capacity and removal efficiency of CAD is evaluated by changing the dosage from 0.05 to 0.30 g, the results are shown in Figure S1 (see Figure S1 in the Supporting Information, available with the online version of this paper). With the increase in the dosage, the removal rate quickly increased, because the CAD provided more adsorption sites and active groups for Hg(II) ion adsorption. When the dosage of the CAD was more than 0.15 g, the adsorption capacity decreased rapidly, the removal efficiency increased relatively slowly, and the adsorption surface of CAD might gradually reach the saturation state. In addition, considering the actual application of the cost, 0.15 g is the optimal value of adsorbent dosage.

Regeneration of adsorbent

The desorption experiments were carried out to study the regeneration and stability of adsorbent. CAD separated from mercury solution after adsorption was placed in 100 ml of saturated EDTA solution, and the mixture was stirred for 3 h. Finally, the concentration of mercury ions was detected by dithizone spectrophotometry. The CAD was reused in four successive adsorption-regeneration cycles; the adsorption capacity decreased from 102 to 82 mg/g after the cycle of five times, indicating that CAD had a good regeneration performance.

Sorption kinetics

In order to more accurately describe the adsorption mechanism of the adsorption process and control the residual time of the whole adsorption process, it was necessary to study the dynamics of Hg(II) ions' adsorption onto CAD. The pseudo-first-order and pseudo-second-order kinetic equations are illustrated in Equations (5) and (6):

$$\ln(q_e - q_t) = \ln q_e - k_1 t \tag{5}$$

$$\frac{t}{q_t} = \frac{1}{k_2 q_e^2} + \frac{1}{q_t} t \tag{6}$$

Here t (min) is the contact time, q_e (mg/g) and q_t (mg/g) are the adsorption capacity at equilibrium and at contact time t, and k_1 and k_2 represent the first and second-order kinetic rate constants.

The experimental adsorption data of the contact time at the temperatures of 25, 35 and 45 °C were fitted by the pseudo-first-order kinetic model and pseudo-second-order kinetic model. The linear plots and adsorption kinetic parameters of the first and second-order model were clearly shown in Figure 5 and Table 2; compared with the pseudo-first-order model, the pseudo-second-order kinetic model fitted the experimental data better. Specifically, the value of calculated qe from the pseudo-second-order model was consistent with the experimental one, and the values of correlation coefficient ($R^2 > 0.995$) were relatively higher for the adsorbent, which suggested the process of Hg(II) ion adsorption onto the CAD followed the pseudo-second-order kinetic model.

Sorption isotherm models

In this study, the influence of the initial Hg (II) ion concentration on the adsorption capacity was explored by changing the initial Hg(II) ion concentration from 100 to 300 mg/L, which is shown in Figure S2 (see Figure S2 in the Supporting Information, available with the online version of this paper) and the experimental adsorption data of the equilibrium adsorption concentration and adsorption capacity of CAD were fitted by the Freundlich and Langmuir models. The equations of the Freundlich and Langmuir models are

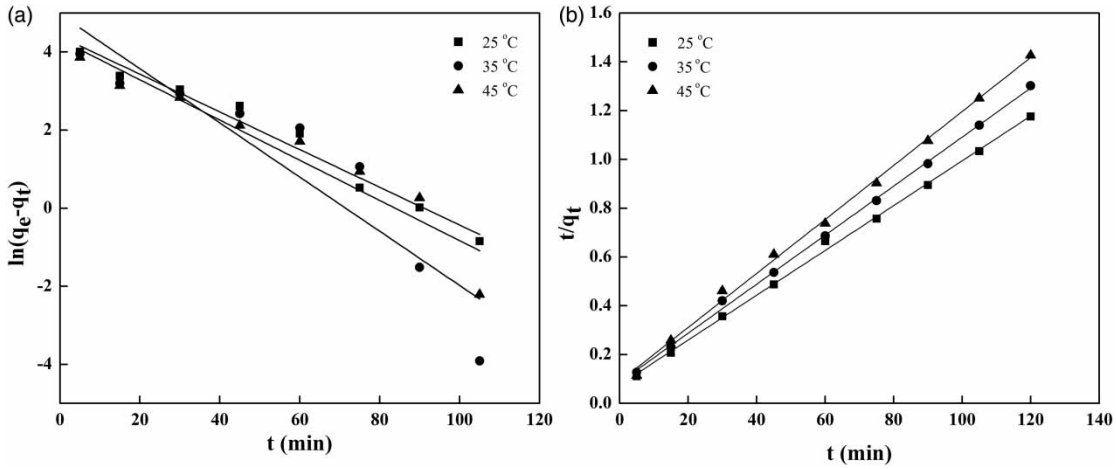

Figure 5 | Pseudo-first-order (a) and pseudo-second-order kinetic plots (b) at different temperatures for the sorption of Hg(II) ions (200 mg/L initial Hg (II) ion concentration, 100 ml; CAD, 0.15 g; pH, 4; time, 120 min).

Table 2 | Adsorption kinetic parameters of Hg(II) ion adsorption onto the CAD

		The pseudo-first-order model			The pseudo-second-order model		
Temperature (°C)	$q_{e\text{-}exp}$ (mg/g)	$q_{e\text{-}cal}$ (mg/g)	k_1 (min^{-1})	R^2	$q_{e\text{-}cal}$ (mg/g)	k_2 ($g.mg^{-1}.min^{-1}$)	R^2
25	102.01	81.37	0.0483	0.971	109.53	1.08×10^{-3}	0.998
35	92.17	142.86	0.0694	0.84	99.11	1.17×10^{-3}	0.998
45	84.07	75.19	0.0515	0.90	90.01	1.36×10^{-3}	0.999

expressed as Equations (7) and (8):

$$q_e = K_F C_e^{1/n} \tag{7}$$

$$q_e = \frac{q_m K_L C_e}{1 + K_L C_e} \tag{8}$$

where q_e (mg/g) is the adsorption capacity, C_e (mg/L) is the Hg(II) ion concentration at equilibrium, q_m (mg/g) is the maximum adsorption capacity, K_F and K_L expresses the Freundlich and Langmuir adsorption constants, and 1/n expresses the adsorption intensity (dimensionless).

From the nonlinear regression analysis of Freundlich adsorption and Langmuir adsorption models in Figure 6, the regression coefficients R^2 of Langmuir and Freundlich were calculated to be 0.996 and 0.840, and the values of q_m (110 mg/g) determined of Langmuir adsorption model were mainly consistent with experimental one (102 mg/g), which suggested that Langmuir equation fitted better than Freundlich equation. The Langmuir isotherm is based on monolayer sorption onto a sorbent surface containing a limited number of adsorptive sites with uniform energies. Results indicate the surfaces of CAD distribute uniform functional groups (hydroxy, amino) and the adsorption mechanism for Hg(II) ions is controlled monolayer adsorption.

Sorption thermodynamics

To investigate the effect of temperature on the adsorption of Hg(II) ions onto CAD, adsorption experiments were carried out with the temperature set at 25, 35 and 45 °C. According to Equations (9) and (10), thermodynamic parameters such as the changes in Gibbs free energy (ΔG), enthalpy (ΔH°) and entropy (ΔS°) were calculated by analysis of experimental data.

$$\ln\left(\frac{q_e}{C_e}\right) = \frac{-\Delta H^0}{RT} + \frac{\Delta S^0}{R} \tag{9}$$

$$\Delta G^0 = -RT \cdot \ln\left(\frac{q_e}{C_e}\right) \tag{10}$$

According to Equation (9), the graph of $\ln(q_e/C_e)$ versus 1/T was a straight line in Figure 7, $\ln(q_e/C_e)$ values were plotted against 1/T with slope and intercept equal to $\Delta H^0/R$ and $\Delta S^0/R$, ΔH^0 (−25.49 kJ/mol), ΔS^0 (−79.23 J/mol) were

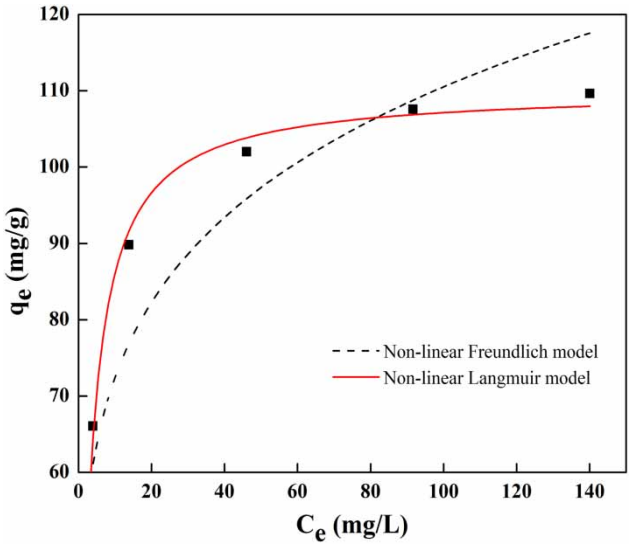

Figure 6 | Nonlinear Langmuir and nonlinear Freundlich isotherm plots for the sorption of Hg (II) ions.

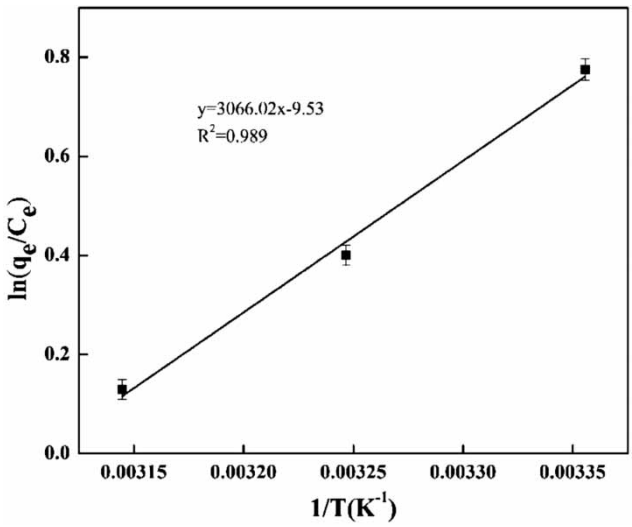

Figure 7 | Plot dependence of ln(qe/Ce) on 1/T for the estimation of thermodynamic parameters (200 mg/L initial Hg (II) ion concentration, 100 ml; CAD, 0.15 g; pH, 4; time, 120 min).

obtained. Values of ΔG were calculated to be −1.92, −1.03 and −0.34 kJ/mol for 25, 35 and 45 °C according to Equation (10), which suggested adsorption of Hg(II) ions onto CAD was a feasible and spontaneous exothermic process due to negative values of ΔH^0 and ΔG°.

Comparison with other studies

Table S1 (see Table S1 in the Supporting Information, available with the online version of this paper) shows a comparison of our results and other reported data on the adsorption capacity (q_{max}) of Hg(II) ions. According to Table S1, the adsorption capacity is more excellent than that of most adsorbents. The possible mechanism of Hg (II) ion adsorption onto CAD can be described below; active sites such as the hydroxyl (−OH) and amino group ($-NH_2$) from CAD are responsible for metal ions' adsorption by forming coordination bonds with Hg (II) ions. The chelating mechanism is expressed as follows (Equations (11) and (12)) (Kyzas & Bikiaris 2015):

$$(CAD)-NH_2+Hg^{2+}+(CAD)-NH_2 \leftrightarrow (CAD)-NH_2\cdots Hg^{2+}\cdots H_2N-(CAD) \quad (11)$$

$$(CAD)-OH+Hg^{2+}+(CAD)-OH \leftrightarrow (CAD)-OH\cdots Hg^{2+}\cdots HO-(CAD) \quad (12)$$

In addition, taking into account the cost of diatomite, CAD will be a good candidate for applications in heavy metal removal from wastewater.

CONCLUSION

In summary, with glutaraldehyde as the bridge, the amino-modified diatomite and CS were linked in the form of chemical bonds to synthesize the adsorbent CAD, which makes the CAD stable. The optimum adsorption conditions were obtained by systematically optimizing the relational parameters of adsorption; the maximum adsorption capacity of Hg(II) ions reached 102 mg/g with the optimum pH value of 4 and 120 min contact time at 25 °C. It was found that the adsorption experiment data of CAD followed the secondary adsorption kinetics and Langmuir isothermal adsorption model, and the sorption process of the Hg(II) ions onto the CAD was based on monolayer chemical adsorption. The negative ΔG^0 and ΔH^0 indicated that the adsorption was a feasible and spontaneous exothermic process. In summary, CAD will be an environmental and cost-effective adsorbent applied in the fields of Hg(II) ion adsorption with special chemical and physical adsorption properties.

ACKNOWLEDGEMENTS

The authors are grateful to the Fundamental Research Funds for the Central Universities (N160504001).

REFERENCES

Al-Ghouti, M. A., Khraisheh, M. A. & Tutuji, M. 2004 Flow injection potentiometric stripping analysis for study of adsorption of heavy metal ions onto modified diatomite. *Chemical Engineering Journal* **104** (1), 83–91.

Amor, Z., Bariou, B., Mameri, N., Taky, M., Nicolas, S. & Elmidaoui, A. 2001 Fluoride removal from brackish water by electrodialysis. *Desalination* **133** (3), 215–223.

Awual, M. R., Hasan, M. M., Eldesoky, G. E., Khaleque, M. A., Rahman, M. M. & Naushad, M. 2016 Facile mercury detection and removal from aqueous media involving ligand impregnated conjugate nanomaterials. *Chemical Engineering Journal* **290**, 243–251.

Bailey, S. E., Olin, T. J., Bricka, R. M. & Adrian, D. D. 1999 A review of potentially low-cost sorbents for heavy metals. *Water Research* **33** (11), 2469–2479.

Bello, O. S., Adegoke, K. A. & Oyewole, R. O. 2014 Insights into the adsorption of heavy metals from wastewater using diatomaceous earth. *Separation Science & Technology* **49** (12), 1787–1806.

Caner, N., Sarı, A. & Tüzen, M. 2015 Adsorption characteristics of mercury(ii) ions from aqueous solution onto chitosan-coated diatomite. *Industrial & Engineering Chemistry Research* **54** (30), 7524–7533.

Carter, K. P., Young, A. M. & Palmer, A. E. 2014 Fluorescent sensors for measuring metal ions in living systems. *Chemical Reviews* **114** (8), 4564–4601.

Charerntanyarak, L. 1999 Heavy metals removal by chemical coagulation and precipitation. *Water Science and Technology* **39** (10–11), 135–138.

Chen, H. B., Wang, D. B., Li, X. M., Yang, Q., Luo, K., Zeng, G. M. & Tang, M. L. 2014 Effects of Cd(II) on wastewater biological nitrogen and phosphorus removal. *Chemosphere* **117** (1), 27–32.

Cheng, H. & Hu, Y. 2012 Mercury in municipal solid waste in China and its control: a review. *Environmental Science & Technology* **46** (2), 593–605.

Cho, E. S., Kim, J., Tejerina, B., Hermans, T. M., Jiang, H., Nakanishi, H., Yu, M., Patashinski, A. Z., Glotzer, S. C., Stellacci, F. & Grzybowski, B. A. 2012 Ultrasensitive detection of toxic cations through changes in the tunnelling current across films of striped nanoparticles. *Nature Materials* **11** (11), 978–985.

Demirbas, A., Pehlivan, E., Gode, F., Altun, T. & Arslan, G. 2005 Adsorption of Cu(II), Zn(II), Ni(II), Pb(II), and Cd(II) from aqueous solution on amberlite IR-120 synthetic resin. *Journal of Colloid & Interface Science* **282** (1), 20–25.

Etemadi, M., Samadi, S., Yazd, S. S., Jafari, P., Yousefi, N. & Aliabadi, M. 2017 Selective adsorption of Cr (VI) ions from aqueous solutions using Cr (VI)-imprinted Pebax/chitosan/GO/APTES nanofibrous adsorbent. *International Journal of Biological Macromolecules* **95**, 725–733.

Fan, L., Luo, C., Sun, M., Li, X. & Qiu, H. 2013 Highly selective adsorption of lead ions by water-dispersible magnetic chitosan/graphene oxide composites. *Colloids and Surfaces B: Biointerfaces* **103**, 523–529.

Gökalp, N., Ulker, C. & Güvenilir, Y. 2016 Enhancing the properties of *Candida antarctica* lipase B by immobilization on precipitated silica modified with 3-aminopropyltriethoxysilane (APTES). *New Biotechnology* **33**, S106–S106.

Kadirvelu, K., Thamaraiselvi, K. & Namasivayam, C. 2001 Removal of heavy metals from industrial wastewaters by adsorption onto activated carbon prepared from an agricultural solid waste. *Bioresource Technology* **76** (1), 63–65.

Khraisheh, M. A., Al-Degs, Y. S. & McMinn, W. A. 2004 Remediation of wastewater containing heavy metals using raw and modified diatomite. *Chemical Engineering Journal* **99** (2), 177–184.

Kyzas, G. Z. & Bikiaris, D. N. 2015 Recent modifications of chitosan for adsorption applications: a critical and systematic review. *Marine Drugs* **13** (2015), 312–337.

Li, B., Zhang, Y., Ma, D., Shi, Z. & Ma, S. 2014 Mercury nano-trap for effective and efficient removal of mercury (II) from aqueous solution. *Nature Communications* **5**, 5537.

Naushad, M., Alothman, Z. A., Awual, M. R., Alam, M. M. & Eldesoky, G. E. 2015 Adsorption kinetics, isotherms, and thermodynamic studies for the adsorption of Pb^{2+}, and Hg^{2+}, metal ions from aqueous medium using Ti(IV) iodovanadate cation exchanger. *Ionics* **21** (8), 2237–2245.

Qiao, B., Wang, T. J., Gao, H. & Jin, Y. 2015 High density silanization of nano-silica particles using γ-aminopropyltriethoxysilane (APTES). *Applied Surface Science* **351**, 646–654.

Reddy, D. & Lee, S. M. 2013 Application of magnetic chitosan composites for the removal of toxic metal and dyes from aqueous solutions. *Advances in Colloid and Interface Science* **201**, 68–93.

Sheng, G., Wang, S., Hu, J., Lu, Y., Li, J., Dong, Y. & Wang, X. 2009 Adsorption of Pb (II) on diatomite as affected via aqueous solution chemistry and temperature. *Colloids and Surfaces A: Physicochemical and Engineering Aspects* **339** (1), 159–166.

Sun, J., Yang, Q., Wang, D., Wang, S., Chen, F., Zhong, Y., Yi, K., Yao, F., Jiang, C., Li, S., Li, X. & Zeng, G. 2017 Nickel toxicity to the performance and microbial community of enhanced biological phosphorus removal system. *Chemical Engineering Journal* **313**, 415–423.

Wu, J., Yang, Y. S. & Lin, J. 2005 Advanced tertiary treatment of municipal wastewater using raw and modified diatomite. *Journal of Hazardous Materials* **127** (1), 196–203.

Xu, Q., Li, X., Ding, R., Wang, D., Liu, Y., Wang, Q., Zhao, J., Chen, F., Zeng, G., Yang, Q. & Li, H. 2017 Understanding and mitigating the toxicity of cadmium to the anaerobic fermentation of waste activated sludge. *Water Research* **124**, 269–279.

Yu, Y., Addai-Mensah, J. & Losic, D. 2012 Functionalized diatom silica microparticles for removal of mercury ions. *Science and Technology of Advanced Materials* **13** (1), 15008–15018.

First received 26 September 2017; accepted in revised form 24 December 2017. Available online 10 January 2018